Seismic reservoir characterization of Utica-Point Pleasant Shale with efforts at quantitative interpretation — A case study: Part 1

Satinder Chopra[1], Ritesh Kumar Sharma[1], Hossein Nemati[2], and James Keay[2]

Abstract

The Utica Shale is one of the major source rocks in Ohio, and it extends across much of the eastern United States. Its organic richness, high content of calcite, and development of extensive organic porosity make it a perfect unconventional play, and it has gained the attention of the oil and gas industry. The primary target zone in the Utica Play includes the Utica Formation, Point Pleasant Formation, and Trenton Formation intervals. We attempt to identify the sweet spots within the Point Pleasant interval using 3D seismic data, available well data, and other relevant data. This has been done by way of organic richness and brittleness estimation in the rock intervals. The organic richness is determined by weight % of total organic carbon content, which is derived by transforming the inverted density volume. Core-log petrophysical modeling provides the necessary relationship for doing so. The brittleness is derived using rock-physics parameters such as the Young's modulus and Poisson's ratio. Deterministic simultaneous inversion along with a neural network approach are followed to compute the rock-physics parameters and density using seismic data. The correlation of sweet spots identified based on the seismic data with the available production data emphasizes the significance of integration of seismic data with all other relevant data.

Introduction

The Marcellus Shale, which has become widely known as a source of natural gas in the eastern United States, is a thick formation that covers 95,000 mi^2 across the Appalachian Basin. The first well that used horizontal fracturing technology for completion in the Marcellus shale was drilled in 2006 by Range Resources (Pickett, 2015). The formation contains 500 Tcf of estimated recoverable gas reserves. Approximately 2000–7000 ft below the Marcellus sits the geographically even more massive formation, the Utica Shale (Figure 1). Its areal extent is larger in that it spans over 170,000 mi^2 over portions of seven U.S. states (Pennsylvania, Ohio, West Virginia, New York, Virginia, Kentucky, and Tennessee) and across the border into Canada (Ontario) (EIA Report, 2017). The Utica Shale is considered a source rock for oil and natural gas, and it has been produced by conventional means in the overlying rock formations. According to a 2012 USGS report, the formation holds 940 million barrels of oil and approximately 38 Tcf of natural gas (Kirschbaum et al., 2012), but with more drilling and production, these estimates have been revised and stand at 2 billion barrels of oil and 782 Tcf of natural gas (Cocklin, 2015).

Eastern Ohio has now become a new drilling target and the focus of development activity in the Utica Shale play, followed by western Pennsylvania. The main reason for this is that the thermal maturity studies of the Utica Play Shales have indicated a northeast–southwest trend over eastern Ohio and western Pennsylvania, with a western oil phase window, a central wet gas phase window, and an eastern dry gas phase window (Mariani, 2013). The oil and wet gas phase windows span a large part of eastern Ohio and a small corner of northwestern Pennsylvania (Figure 2). In this respect, Utica is considered analogous to the Eagle Ford Shale in Texas. The other significant reason is that the Utica Play thins to the west in Ohio and becomes deeper and thicker as its dips to the east and southeast of the Appalachian Basin (Antoine and Frederic, 2016). In eastern Ohio, therefore, the Utica Play is the preferred target (over the Marcellus) due to its increased thickness within the oil and wet gas windows and the higher reservoir pressures present because of the extra 2000–6000 ft of burial.

One of the key elements for a successful shale resource play is its thickness. The thickness of the Utica Shale in eastern Ohio is greater than 200 ft. As mentioned earlier, it thins to the west and northwest, and the thickness increases to greater than 500 ft as it dips to the southeast.

Historically, the early vertical wells that pierced through the Utica, and encountered natural fractures, either showed or produced hydrocarbons. It was not

[1]TGS, Calgary, Canada. E-mail: satinder.chopra@tgs.com; rsharma@arcis.com.
[2]TGS, Houston, Texas, USA. E-mail: mnemati@arcis.com; james.keay@tgs.com.

Manuscript received by the Editor 31 July 2017; revised manuscript received 11 October 2017; published ahead of production 15 December 2017; published online 16 March 2018. This paper appears in *Interpretation*, Vol. 6, No. 2 (May 2018); p. T313–T324, 17 FIGS.
http://dx.doi.org/10.1190/INT-2017-0134.1.

until the first horizontal well was drilled in the Utica that its potential for hydrocarbon production was established. The area has drawn significant exploration attention since then. Even though many companies entered Ohio with the goal of drilling the Marcellus, gradually their strategic planning shifted to drilling the Utica in the liquid-rich areas. Since then, these operating companies have gradually acquired acreages in the liquid-rich areas in eastern Ohio, and they have been producing the liquid-rich gas and primary oil.

In this case study, we present our attempts at reservoir characterization of the Utica — Point Pleasant package in eastern Ohio. Beginning with the geologic setting of the area, we go on to discuss the data that are available for the exercise and then describe the workflow followed. The goal of seismic reservoir characterization is essentially the identification of sweet spots that represent the most favorable drilling areas. Such an exercise entails understanding the elastic properties of the reservoir intervals, lithology, fluid content, and their areal distribution. A good starting point for doing this is to use the available well data and understand the parameters that populate the reservoir intervals at the location of the wells. The sonic, density, gamma ray, resistivity, and porosity log curves were sought for the available wells within the 3D seismic volume. Core analysis results, geochemical as well as geomechanical data, were available for one well. The outcome of this technique should be supplemented with an understanding of faults and fractures in the area and the zone of interest, which in our case is the interval between the Trenton Limestone and Utica Shale. We make use of coherence and curvature attributes for achieving this objective.

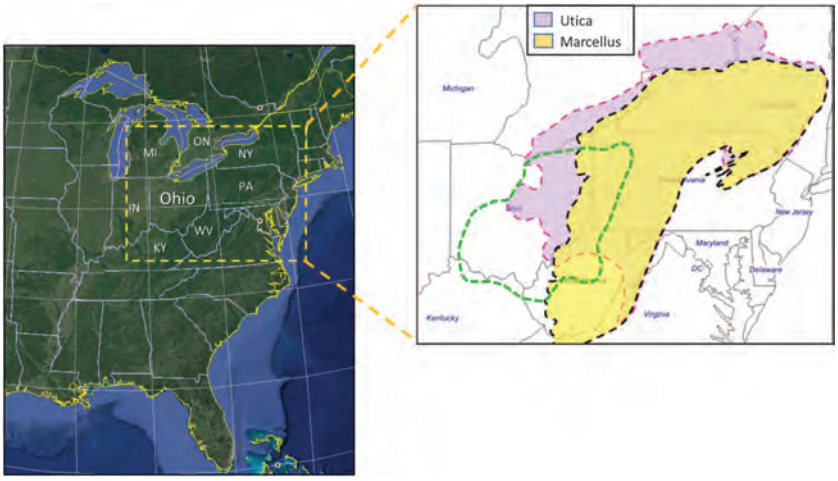

Figure 1. Map of eastern United States showing Ohio and the adjoining states. (Image generated using Google Earth.) The spread of Utica and Marcellus shales are shown in the blowout. (Data source for Utica and Marcellus: EIA.) The outline in green is the extent of Point Pleasant. (Data source: Jefferies, 2013.)

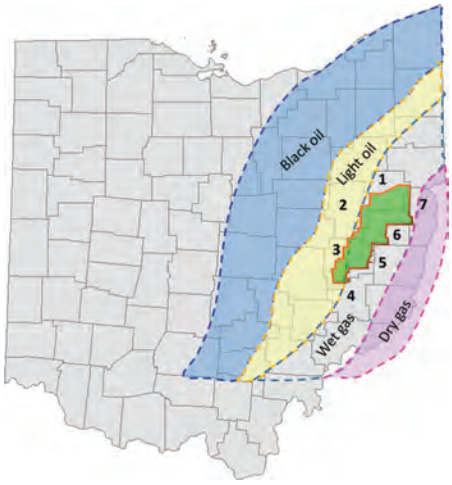

Figure 2. Outline map of Ohio State showing the location of the 3D seismic survey used in the study. The numbers 1–7 show the individual counties discussed in the text over which the 3D seismic survey was shot. The different hydrocarbon phase windows are overlaid on the outline, showing that the survey falls in the wet gas/light oil window. The data for the hydrocarbon phase ribbons were adapted from Mariani (2013).

Geologic setting

Because the Utica and the Marcellus Formations are geographically present over large areas, it is difficult to present a representative stratigraphic column that would be correct everywhere. In Figure 3, we show one that is representative of eastern Ohio and focus on the stratigraphic column from the Black River Group upward (the dark blue arrow in Figure 3), which is primarily fine-grained limestone that was deposited in subtidal environments (Hansen, 1997). Overlying the Black River Group is the Trenton Limestone (the green arrow). Its equivalent to the south is referred to as the Lexington Limestone of Kentucky, which was deposited in an open-shelf marine environment deeper than those of the Black River Group (Hansen, 1997). The Trenton Limestone is dark-gray to brown fossiliferous limestone that includes thin gray to black beds of shale and also has abundant zones of secondary dolomitization.

Above the Trenton Limestone sits the Point Pleasant Formation, which is a black organic-rich crystalline limestone interlayered with black organic-rich shale. The relative amount of limestone in the Point Pleasant Formation decreases toward the top of the formation, and the shale becomes light to dark gray. It is so named because this formation is exposed near the Clermont County town of Point Pleasant in southern Ohio. The Utica shale overlies the Point Pleasant (purple arrow), which is also organic rich. It is light gray to black calcareous shale with lesser limestone layers, and it is denser than Point Pleasant. The Point Pleasant has gradational

contacts between the underlying Trenton Limestone and the overlying Utica Shale.

The interlayering within the Point Pleasant is again a result of Upper Ordovician (open marine) deposition in varying sea levels. The Point Pleasant Formation is shallower and thinner in central Ohio and becomes deeper and thicker in the southeast direction. The oil, condensate, and gas window ribbons trending in the northeast–southwest direction (Figure 2) span through the Point Pleasant and Utica Formations in eastern Ohio, and therefore, it has been the center of drilling activity over the past five years. By 2015, more than 1000 wells had been drilled with greater than 50% of them producing, the remaining waiting on production facilities and gather lines (Downing and Livingston, 2015).

The Utica is overlain by a thick unit of interbedded limestones and shales called the Cincinnati series that appears monotonous. This unit represents a transgressive sequence wherein the shale-dominated subunits reflect deposition in deeper, quieter waters, and the limestone-dominated subunits represent deposition in clearer, shallower waters. The Cincinnati group is overlain by the "Clinton" sandstone (yellow arrow), Salina group, and the Onondaga limestone units.

The Clinton Sandstone Formation of Early Silurian age is present under 25 counties in eastern Ohio, and large quantities of oil and gas have been produced from it. The depth of the Clinton Sandstone increases from the northwest to the southeast. The regional structure is monoclonal dipping S60°E at approximately 50 ft per mile. Its color varies from light gray to reddish (due to the presence of hematite), it may have a thickness of as much as 85 ft, and it becomes more calcareous to the south. It thins to the west and is a shale beyond central Ohio. Horizontal wells with 2000 ft laterals are commonly drilled into the Clinton Sandstone. Although they are more expensive than vertical wells, they yield greater production.

The Bass Islands and Salina Group were deposited in a shallow-water environment during continental elevation, accompanied by a regressing sea in the Late Silurian. Shallow basins at the time experienced salt and gypsum deposition due to the solar evaporation of seawater. The Salina Group consists of basal red and green shales and interbedded salt, anhydrite, dolomite, shale, and upper layers of shale, dolomite, and gypsum. This unit is close to 800 ft thick in places.

Overlying these Silurian rocks are the rocks of Devonian age that are of marine origin. These are the Ohio Shale, Olentangy Shale, the Marcellus Shale (the light blue arrow in Figure 3), Onandaga Limestone, and Oriskany Sandstone. The thickness of this section is up to 4000 ft in western Pennsylvania. Overlying the Devonian system are the Mississippian rocks of shallow water deposition, wholly marine in origin and up to 300 ft in thickness. This includes the Maxwell Limestone, Berea Sandstone, and the Bedford. The shallow marine Berea sandstone is well-known in Ohio. Its average thickness is approximately 45 ft, it is seen as outcrops in quarries in many places, and it is used as building stone. It has produced oil from shallow wells drilled down to 2000 ft.

A significant clarification may be made here. Because Point Pleasant has lower clay content (clay content in Utica is between 30% and 40% but is between 5% and 20% in the Point Pleasant), higher organic content (total organic carbon [TOC] 1%–4%), and better porosity (2%–12%) (Murphy et al., 2013), it has become a more attractive drilling target. The Ohio Department of Natural Resources has carried out various regional studies in the state, and one of them is the TOC content distribution within the Utica, Point Pleasant, and other intervals (Wickstrom, 2013). It is interesting to note that the area covered by the different hydrocarbon phase ribbons shown in Figure 2 fall in the "very good" (2–4 TOC max-wt%) to "excellent" (> 4 TOC max-wt%) pockets of TOC. The Utica serves as a cap rock that helps maintain fluid pressure within Point Pleasant, and it limits fracture propagation within it.

The composite Utica/Point Pleasant package is present over most of Ohio, western Pennsylvania, and the northern part of Western Virginia, but the area in eastern Ohio spans the oil to dry gas window. This is the reason that it is mapped as Utica-Point Pleasant combo over eastern Ohio.

3D seismic data acquisition and processing

The acquisition of a 702 mi^2 (1818 km^2) 3D seismic survey spread over (1) Carroll, (2) Tuscarawas, (3) Guernsey, (4) Noble, (5) Belmont, (6) Harrison, and

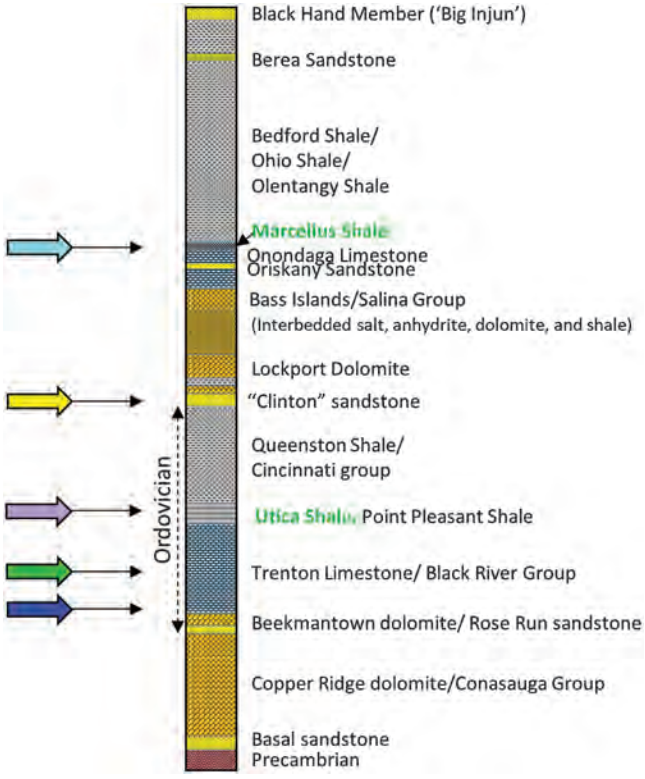

Figure 3. Stratigraphic column for eastern Ohio.

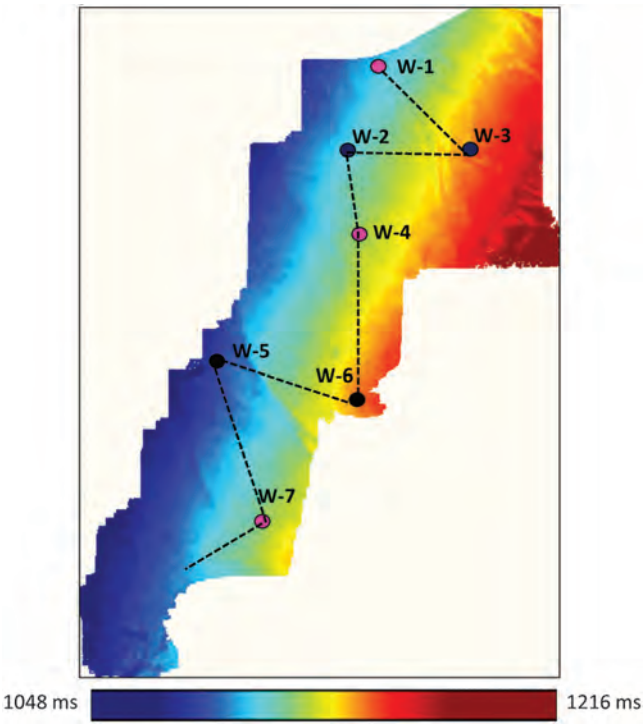

Figure 4. Picked horizon at the Point Pleasant level indicating the dipping reflections from northwest to southeast. The locations of the available wells 1–7 are also indicated.

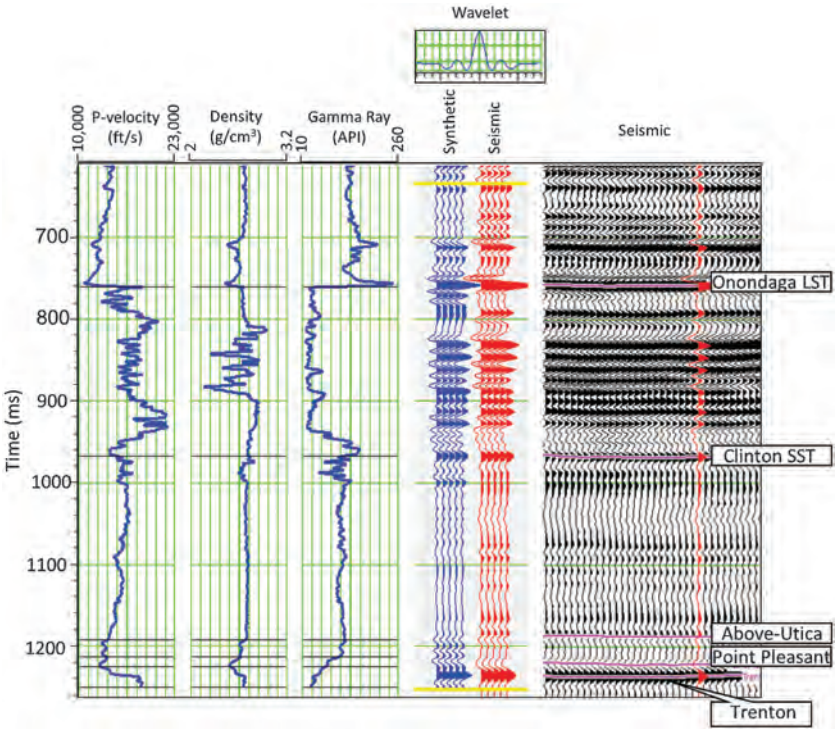

Figure 5. Correlation of well W-3 P-wave velocity, density, and gamma ray curves with seismic data. Notice the sharp impedance contrast seen at the Onondaga Limestone and Trenton Formation levels giving rise to strong reflections. The horizons corresponding to Onondaga Limestone, "Clinton" Sandstone and Point Pleasant and Trenton levels are pickable and seen clearly on the seismic. (Data courtesy TGS, Houston.)

(7) Jefferson counties of eastern Ohio, was completed in late 2015. The location of the survey is shown in Figure 2 (with the counties marked counterclockwise as 1 to 7) and falls in the wet gas and light oil windows of the Utica-Point Pleasant. The acquisition parameters included 220 ft (67.1 m) for source and receiver intervals, 660 ft (201.2 m) for receiver line spacing, 1320 ft (402 m) source line spacing, maximum offset as 19,186 ft (5847.9 m), 2 ms sample interval, 5 s record length, which yielded a bin size of 110 × 110 ft (33.5 × 33.5 m). Two vibrator sweeps of 16 s were used as the seismic source. The processing of this large data volume was completed in June 2016, with anisotropic prestack time migration gathers and stacked volume with 5D interpolation made available for reservoir characterization and quantitative interpretation.

Well-log correlation

Correlation of well-log information with 3D surface seismic data is a convenient way to extend the measured rock properties at well locations spatially over the 3D volume.

As we started compiling well data for our study, we realized that the wells with density logs were located in a cluster to the northern part of the survey, and very few wells had sonic and density curves. A frequently encountered situation is when not many wells have shear sonic log curves available. It is always desirable to have a uniform distribution of wells with sonic, density, and other curves (gamma ray, porosity, and resistivity) although sparse because it helps with the generation of a reliable low-frequency impedance model for impedance inversion, as well as for carrying out any neural network analysis for computation of a reservoir property. Besides, any crossplotting carried out on well data located sparsely on a 3D volume and in localized clusters may not be a true representation of relationships between the crossplotted variables. We, therefore, selected wells that had an optimum distribution as shown in Figure 4. Some of the wells located at the edge of the 3D survey were projected a little bit inside because the seismic data close to the edges of the survey are not very trustworthy.

Once the final seismic data were loaded on the workstation, we assessed its quality and frequency content. The data were preconditioned for random noise attenuation by applying structure-oriented filtering (Marfurt, 2006; Chopra and Marfurt, 2007).

In Figure 5, we show the correlation of the sonic, density, and gamma ray log curves and synthetic seismograms for

well W-3 with the seismic data. Five horizons corresponding to the Trenton Limestone, Point Pleasant, and "Above-Utica" in our zone of interest, as well as the Clinton Sandstone and Onondaga Limestone above it were picked and are indicated in Figure 5. Although the Trenton and Onondaga Limestones show good contrast at their levels on the log curves (and thus prominent reflections on seismic), reflections corresponding to Point Pleasant and Clinton Sandstone were also pickable. But no individual reflection corresponding to the Utica Shale could be picked, and so the closest pickable reflection was considered and called "Above-Utica." A zero-phase wavelet was extracted from the seismic data using a statistical process (shown on the top) and was used for generating the synthetic seismogram. An overall good correlation is seen between the two. A representative seismic section from the 3D seismic volume passing through two wells is shown in Figure 6. A good correlation is seen between the impedance curves and the seismic.

Coherence/curvature attribute application

The preconditioned stacked data were used for horizon picking and also for generating the coherence and curvature attributes. The coherence attribute was generated using the energy-ratio algorithm (Chopra and Marfurt, 2008), and the volumetric multispectral curvature attribute was generated using the algorithm described by Al-Dossary and Marfurt (2006). Horizon slice displays from the most-positive and most-negative curvature volumes are shown in Figure 7. The main faults on the displays, mostly seen north–south, with a prominent one running northwest–southeast, are noticed and indicated with green arrows. In addition to these, there are many smaller lineaments that could be associated with fractures. Such information on networks of naturally occurring fractures is helpful when the results are being compiled, and decisions on drilling targets are made.

Low-frequency trend determination for impedance inversion

The addition of a low-frequency trend forms an important component of the impedance inversion workflow for obtaining absolute values of impedance. Usually, one or more impedance curves are low-pass filtered (<10 Hz) and are used for the generation of a low-frequency impedance model, using interpolation and extrapolation and guided by horizon boundaries. When more than one well is used for the generation of the low-frequency trend, usually an inverse-distance weighted scheme or a process called kriging is used to merge the values across the seismic volume. Such techniques need to be used with care because they can produce artifacts. We instead make use of a relatively new approach for this low-frequency trend generation which considers well-log data and seismic data to establish a relationship between seismic attributes and the available well-log curves. Using the low-frequency model generated with

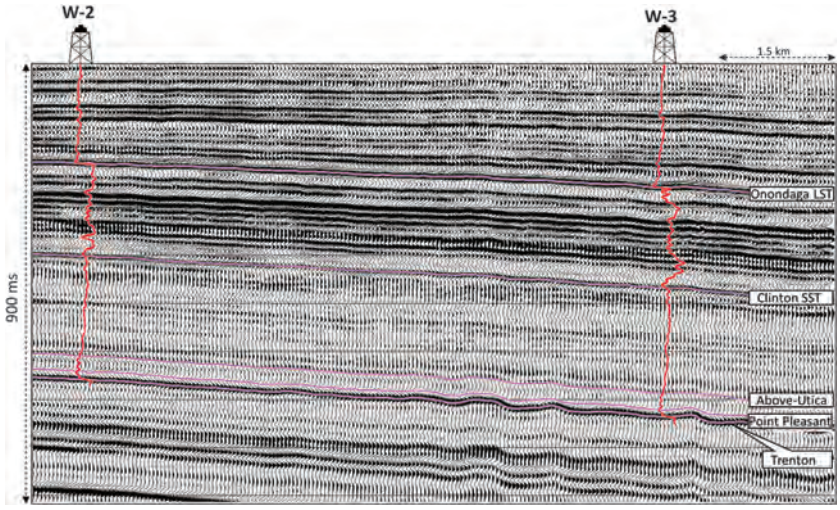

Figure 6. A representative inline running east–west from the 3D seismic volume with P-wave velocity curves (increasing to the right) overlaid on it. The quality of the seismic data is good. The horizons picked on the line show the Onondaga Limestone, "Clinton" Sandstone, Above-Utica, Point Pleasant, and the Trenton to the right. (Data courtesy of TGS, Houston.)

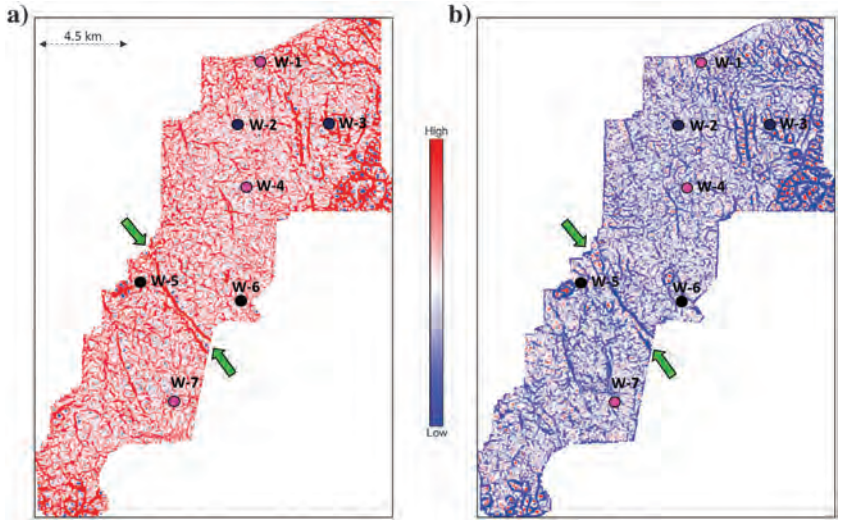

Figure 7. Horizon slice displays midway between the Above-Utica and Point Pleasant markers drawn from the (a) most-positive and (b) most-negative curvature volumes. The lineaments seen in the north–south and northwest–southeast indicate the faults at that level, whereas the many smaller lineaments are suspected to be fractures. (Data courtesy of TGS, Houston.)

a single well as one of the inputs, along with some other seismic data attributes (relative acoustic impedance, instantaneous amplitude, dominant frequency, frequency-filtered seismic data (at 10–20–30–40 and 10–20–50–60 Hz), a multiregression approach (Ray and Chopra, 2015, 2016) is used, wherein a target log is modeled as a linear combination of several input attributes at each sample point. This results in a series of linear equations that are solved by obtaining a linear-weighted sum of the input seismic attributes in such a way that the error between the predicted and the target log is minimized. The choice of the different seismic attributes used could vary, but for the case at hand, we have used the relative acoustic impedance, some instantaneous attributes, and

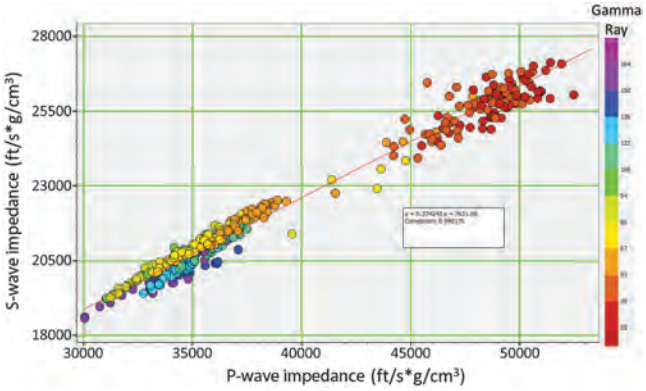

Figure 8. Crossplot of P-wave impedance versus S-wave impedance using well-log data from three wells 1, 4, and 7. A high correlation coefficient is seen for the linear trend observed.

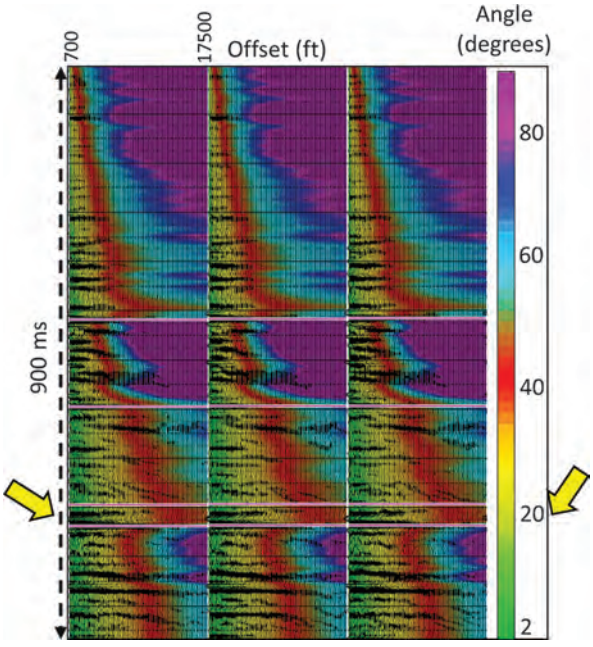

Figure 9. Angle of incidence information overlaid on conditioned gathers. The zone of interest is indicated with yellow arrows. The angle range selected for inversion is 34°. (Data courtesy of TGS, Houston.)

different versions of the filtered seismic data as inputs. Cross-validation of the predicted attributes forms part of the workflow in which one well is withdrawn and is estimated by using the other wells and compared. If the correlation coefficient between the existing and predicted curves is high, which was found to be the case, it lends more confidence to the analysis. This approach results in more accurate low-frequency impedance models. More details can be found in the cited references.

Because shear log curves were available in only three of the eight wells over the 3D survey that had sonic and density logs, we crossplotted the P- and S-impedance for these three wells as shown in Figure 8. The linear relationship seen therein was used to generate the shear curves for five wells that did not have the shear curves, and then we used those seven shear impedance curves (three measured and four predicted using the relationship) for the generation of the low-frequency S-impedance model for inversion. Having determined the low-frequency models for P-wave and S-wave impedance, the next step is to carry out preconditioning of the prestack data for enhancing its signal-to-noise ratio.

Preconditioning of prestack seismic data and simultaneous inversion

The prestack seismic data were preconditioned carefully, making sure that amplitudes were preserved. The preconditioning entailed supergathering (3×3), bandpass filtering, random noise attenuation, and trim statics processes, with difference plots taken at each step to ensure that no useful signal leaked through any of the processes.

The angle of incidence information was extracted from the velocity model generated for carrying out simultaneous inversion and overlaid on the offset gathers as shown in Figure 9. Such a plot helps quality control the range of angles that can be meaningfully used in the

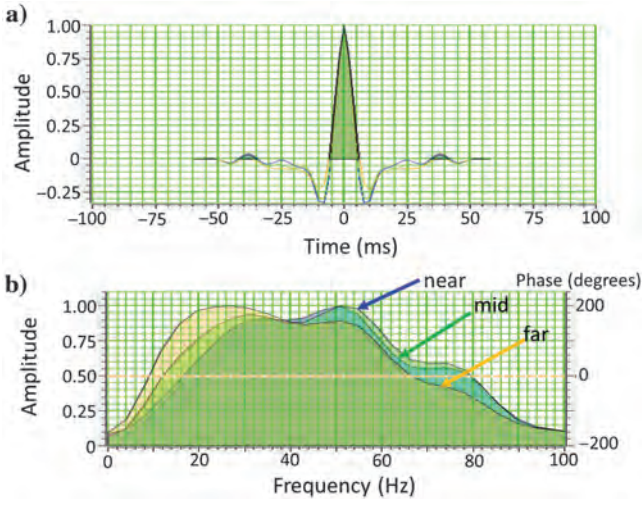

Figure 10. (a) Zero-phase wavelets estimated from near-, mid-, and far-angle stacks, which are to be used in the simultaneous inversion. Their frequency spectra are shown in (b). Notice the variation in the frequency content of these wavelets.

inversion process. We found that the usable angle range for simultaneous inversion was 34°.

In simultaneous prestack impedance inversion, multiple partial angle substacks are inverted simultaneously. For each angle stack, a unique wavelet is estimated (as shown in Figure 10). Subsurface low-frequency models for P-impedance, S-impedance, and density constrained with appropriate horizons in the broad zone of interest, are constructed using the approach explained above. The models, wavelets, and partial stacks were used as input in the inversion, and the output was P-impedance and S-impedance. Because the usable angle range was only 34°, the density attribute could not be determined with simultaneous inversion, which requires angles beyond 40°.

Sweet-spot determination

The main goal for shale resource characterization is usually the identification of sweet spots that represent the most favorable drilling targets. Such sweet spots can be described as those pockets in the target formation that exhibit *high* TOC content, *high porosity*, as well as *high brittleness*. The organic richness in the shale rocks influences properties such as P-wave and S-wave velocities, and density (Chopra et al., 2012). Therefore, attempts have been made to detect changes in TOC from the surface seismic response using impedance and other attributes such as the V_P-V_S ratio, lambda-rho, and mu-rho. (Sharma and Chopra, 2016). In this study, we have tried to bring in data from core analysis, as well as geochemical and geomechanical analysis, and integrate that with surface seismic data. The density and TOC measurements made on the core samples in the Point Pleasant interval were crossplotted as shown in Figure 11. A strong linear relationship is seen between them. This suggests that the density attribute would be required if the organic-rich zones in the Point Pleasant interval are to be determined from seismic data.

In addition as stated above, as the angle range was not favorable for computing density from seismic data through simultaneous inversion, we turned to neural network analysis for its determination. There are two aspects to our motivation for the use of neural networks here. The first is that there were more wells located in the 3D survey that had density logs available than those with density and sonic logs, and so could be used in the neural network analysis. The second aspect has to do with the simultaneous inversion process itself. The simultaneous inversion is based on an incrementally linearized approach in finding the solution (model-based inversion) and is dependent on the choice of the starting impedance model (Ray and Chopra, 2015, 2016). Even though other methods exist that could possibly use a nonlinear minimization of error

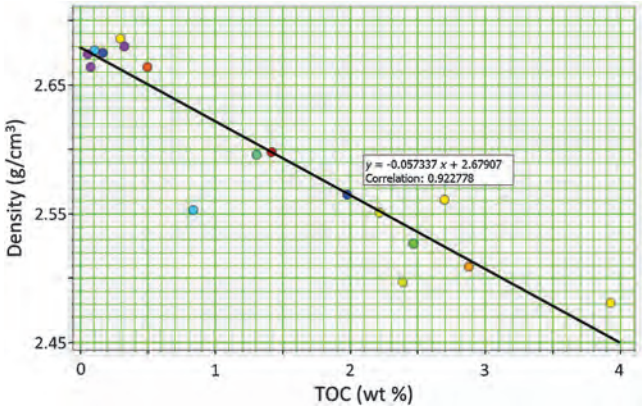

Figure 11. Crossplot of density and weight percent of TOC as determined from core data in the Point Pleasant interval. A good linear relationship is seen between the crossplotted variables.

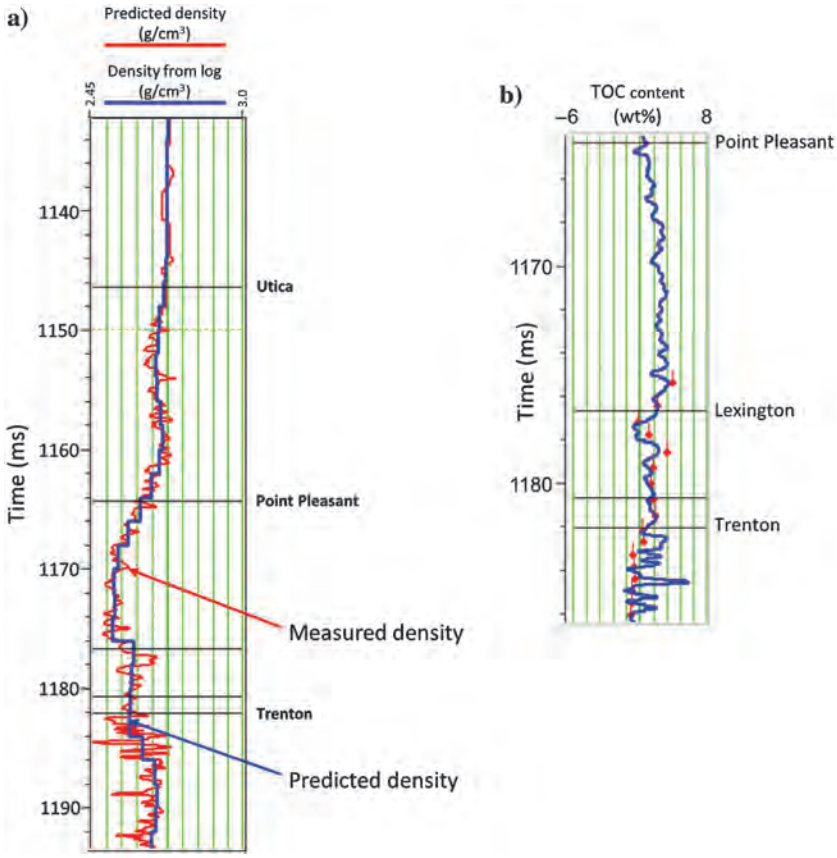

Figure 12. (a) The density trace predicted with neural network application compared with the measured density log curve at the location of well W-7. The two curves overlay well and thus enhance our confidence in neural network density prediction. (b) The derived TOC (wt%) curve shown correlated with the TOC values from the core samples. The good correlation is encouraging.

approach, their applications are still not common. Therefore, we decided to determine density with probabilistic neural network analysis, using among others, some of the attributes determined from simultaneous inversion. The details of the neural network approach followed, as well as some other work with regard to the integration of core, geochemical and geomechanical data, and seismic data are being presented in a companion paper. But in Figure 12, we show how the predicted density compares with the measured density at the location of well W-7. The good match between the curves enhanced our confidence in this approach.

Once the density volume was determined from neural network analysis, the linear relationship shown in Figure 11 was used to transform it to a TOC volume. An arbitrary cross section passing through the different wells as well as a horizon slice at the Point Pleasant level is shown in Figure 13. High TOC content is noticed in the northern part of the survey, which is consistent with TOC trend observed in the Utica-Point Pleasant play (Wickstrom, 2013).

Besides the organic richness consideration, it is vital that reservoir zones are sufficiently brittle because the fracturing potential of a shale reservoir is a fundamental function of its brittleness. Attempts are usually made to identify the brittle zones with the help of Poisson's ratio and Young's modulus as a rock's ability to fail under stress is represented by the former, whereas the ability of sustaining fractures is reflected by the latter (Rickman et al., 2008).

In Figure 14a, we show a crossplot between Young's modulus and Poisson's ratio from well data for wells W-1 and W-7 from the Utica through Point Pleasant to the Trenton interval. We notice a positive correlation between the two parameters. The data points corresponding to low Young's modulus and Poisson's ratio and high Young's modulus and Poisson's ratio are enclosed in the different polygons and back projected onto the log curves (Figure 14b). We notice that the Point Pleasant interval exhibits low Young's modulus ($E\rho$) and low Poisson's ratio relative to the Utica interval. As is seen in many other shale formations, brittleness is found to increase as Poisson's ratio decreases and Young's modulus increases (Rickman et al., 2008). Going by this observation, Point Pleasant does not seem to follow this behavior, even though the production from the multistage fracking in this interval has been established (Patchen and Carter, 2015). Within the Point Pleasant interval (highlighted by the red polygon), we also see a variation in these two parameters. To study the variation of these

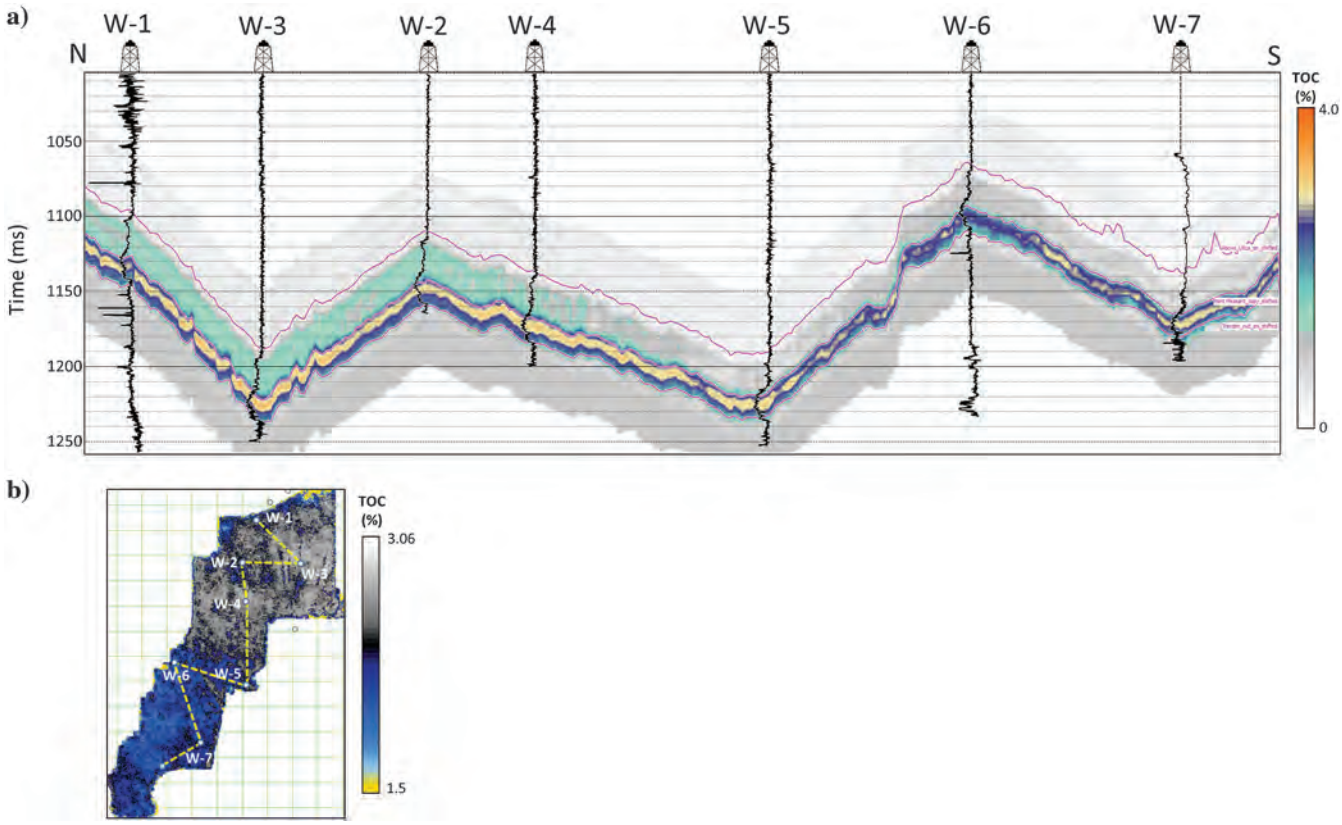

Figure 13. (a) An arbitrary line from the TOC volume and passing through wells W-1 and W-7. (b) A horizon slice at the PP level from the TOC volume. The path followed by the arbitrary line through the different wells is also indicated. The overlaid curves are the density logs. The TOC content appears to be more on the northern side of the line and gradually decreases to the southern side. (Data courtesy of TGS, Houston.)

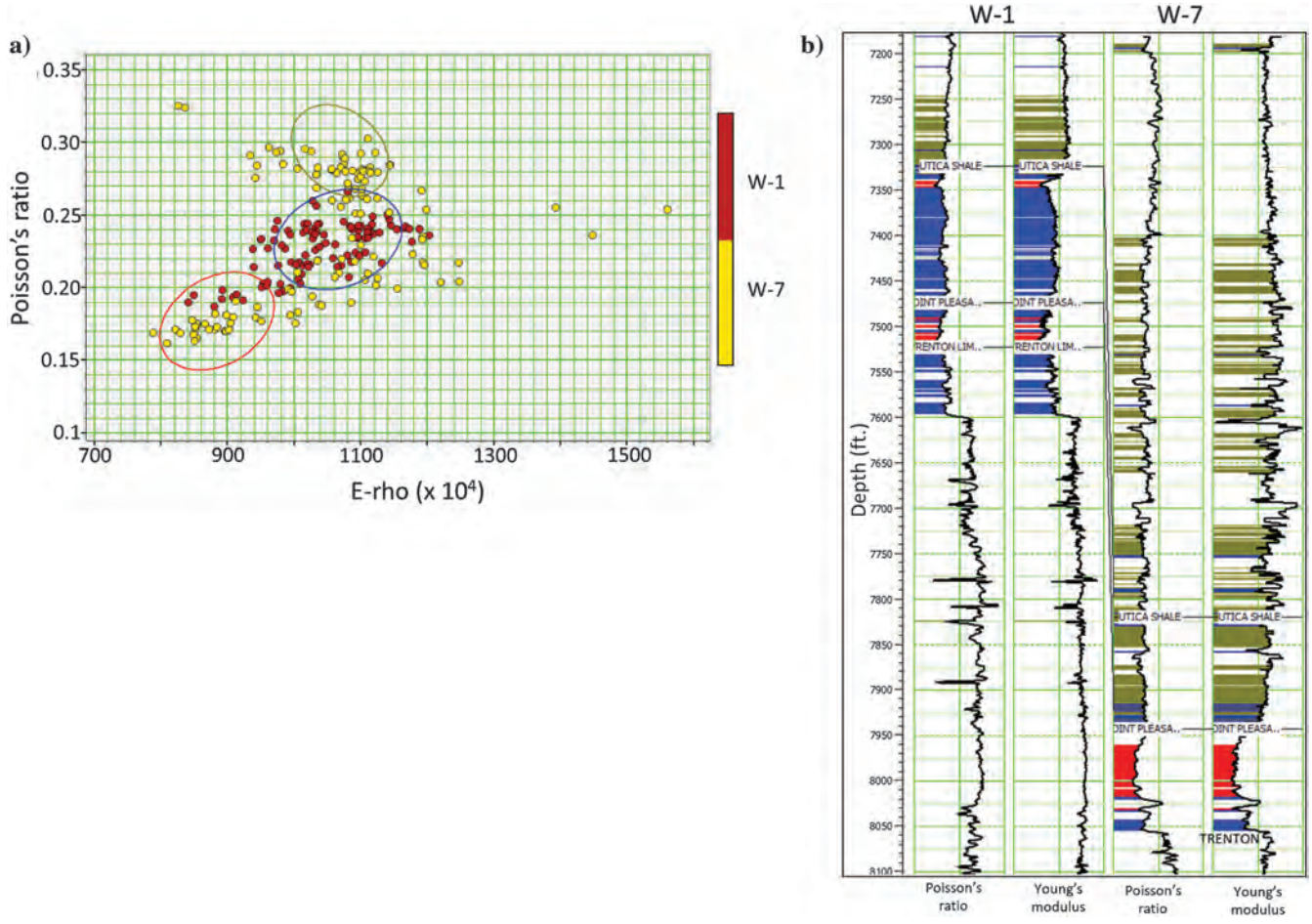

Figure 14. (a) Crossplot between Young's modulus and Poisson's ratio for wells W-1 and W-7 for the Utica to Trenton interval. (b) Back projection of the cluster points in different polygons on log curves. Note the positive correlation between the crossplotted parameters. In addition, we see a variation in the values of both parameters for the points in the red polygon, most of which are coming from the Point Pleasant interval.

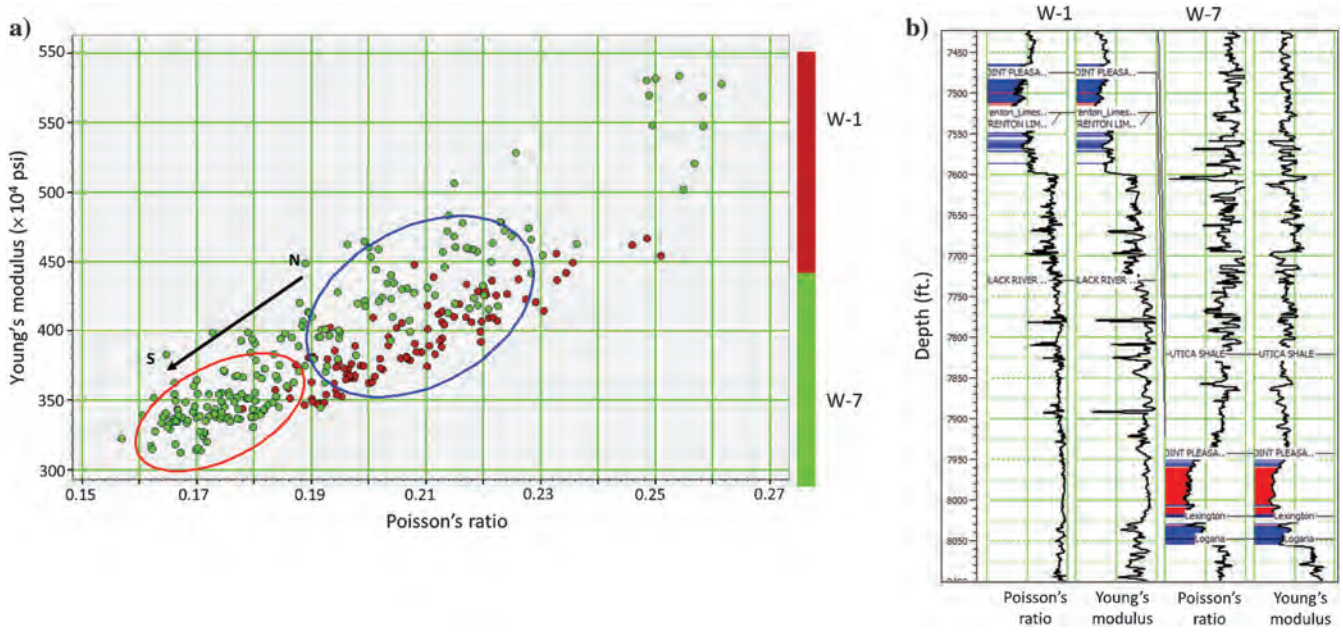

Figure 15. (a) Crossplot between Young's modulus and Poisson's ratio for wells W-1 and W-7 for the Point Pleasant interval to study the variation of the parameters within this interval. (b) The projection of the points enclosed in red and blue polygons shows that the Young's modulus and Poisson's ratio decrease going from well W-1 (north) to well W-7 (south).

parameters within this interval, we restrict the data points coming into the crossplot to just the Point Pleasant interval as shown in Figure 15, and we see the cluster of points enclosed in the red polygon coming from W-7 (to the south) and the ones in the blue polygon coming from W-1 (to the north). Poisson's ratio and Young's modulus decrease going from north to south.

Grieser and Bray (2007) propose computing the brittleness average from the Young's modulus and Poisson's ratio and correctly predict brittle and ductile shale pockets within the Barnett shale by considering all values of Poisson's ratio less than 0.25 as the brittleness threshold and all values of Young's modulus greater than 3.1×10^6 psi as prone to fracturing under stress.

We follow a similar approach and demonstrate its application to the Utica-Point Pleasant play. Realizing that the Point Pleasant interval has high calcite content (Patchen and Carter, 2012), and therefore its ability to fail under stress and sustain fractures must be high, we extracted the P-wave impedance and S-wave impedance derived from simultaneous inversion and density derived from probabilistic neural network analysis to compute the Young's modulus and Poisson's ratio attributes for the seismic volume. These were then crossplotted just for the Utica to Trenton interval as shown in Figure 16. Note that most points below a Poisson's ratio value of 0.23 (enclosed in red and green polygons) come from the Point Pleasant interval. Thus, we interpret this interval to be prone to get fractured under stress. The ability of this interval to sustain fractures in a relative sense can be examined based on the Young's modulus attribute. It can be seen from Figure 16a that the points enclosed by the green polygon correspond to higher values of the Young's modulus, than of the points enclosed by the red polygon. When we project these points on the vertical arbitrary line passing through the wells (shown in Figure 13a) as exhibited in Figure 16b, we notice that the northern side of this line exhibits higher brittleness than the southern side.

To examine the lateral variation in the Young's modulus, we extract a horizon slice from the Young's modulus volume that is shown in Figure 17a. The northern part of the display shows higher values of the Young's modulus. This is consistent with our observation from wells W-1 and W-7 in Figures 14 and 15.

Thus, by restricting the values of the Poisson's ratio and examining the variation of the Young's modulus, we have been able to determine the variation in the brittleness of the Point Pleasant interval. In addition to brittleness, organic richness was also explored for through the TOC volume. For doing this, we draw an equivalent horizon slice from the TOC volume, which is shown in

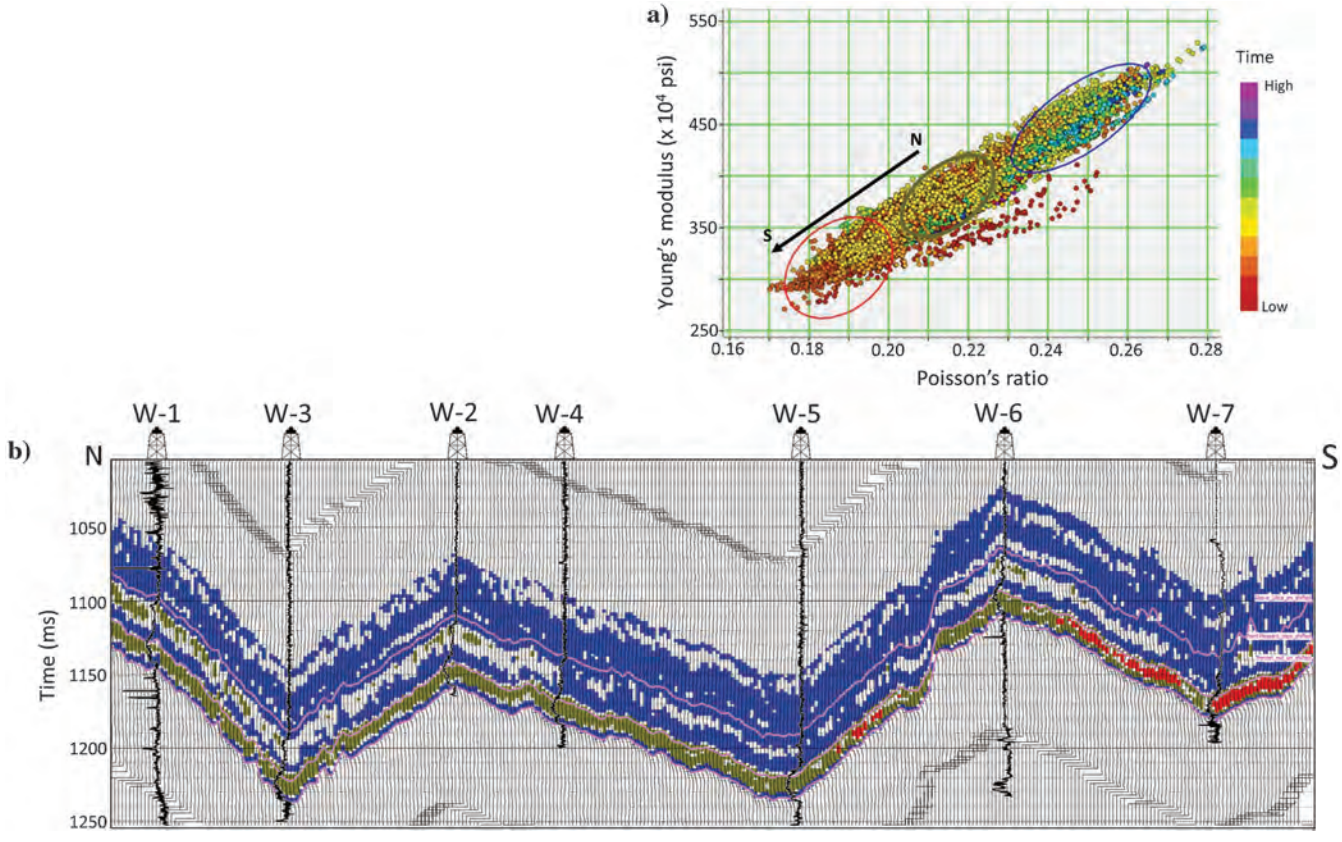

Figure 16. (a) Crossplot between the Young's modulus and Poisson's ratio as derived from seismic data for the Utica to Trenton interval. Notice a similar positive correlation between the crossplotted parameters as seen in Figure 15. (b) The cluster points in different polygons on the crossplot when projected on the vertical show higher brittleness on the northern side of the survey. (Data courtesy of TGS, Houston.)

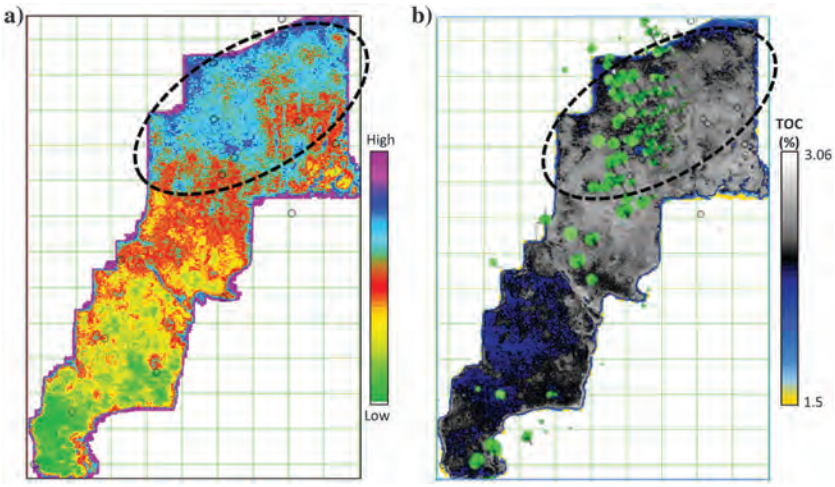

Figure 17. Horizon slices from (a) Young's modulus and (b) TOC volumes, averaged in a 10 ms window in the Point Pleasant interval. The highlighted portions indicate the sweet spots corresponding to high Young's modulus and high TOC. (Data courtesy of TGS, Houston.) The production data are overlaid on the TOC display. It may be mentioned here that the production data have been obtained from the online open database, and we are not sure about its accuracy. However, the match seems convincing.

Figure 17b. We notice relatively higher TOC values in the northern part, even though most of the displayed TOC values are between 2 and 3 wt% (which suggests that more or less the whole survey is rich in TOC values). The areas highlighted in the black polygons are thus the sweet spots that have been determined from the above analysis. This seems accurate enough as confirmed by the available production data overlaid on the TOC display.

We have shown the sweet spots for the Point Pleasant interval within the 3D survey area, but a similar analysis can be carried out for the Utica and the Trenton intervals, which we will try and cover in a companion paper.

Conclusion

We have characterized the Point Pleasant formation in eastern Ohio using 3D surface seismic and its integration with core, geochemical, and geomechanical data. This has been done by deriving rock-physics parameters (Young's modulus and Poisson's ratio) through deterministic simultaneous inversion and neural network analysis. We find that the Point Pleasant Formation does not seem to follow the commonly followed variation in terms of low Poisson's ratio and high Young's modulus for brittle pockets. Instead, by restricting the values of the Poisson's ratio and examining the variation of the Young's modulus, we could determine the brittleness behavior within the Point Pleasant interval. Combining the brittleness behavior with the organic richness determined through the TOC content, we could pick sweet spots in the Point Pleasant interval that match the production data.

Through this case study, we emphasize the integration of 3D surface seismic data with all other relevant data to accurately characterize the Point Pleasant Formation.

Acknowledgements

We wish to thank Arcis Seismic Solutions/TGS for encouraging this work and for the permission to present and publish it.

References

Al-Dossary, S., and K. J. Marfurt, 2006, 3D volumetric multispectral estimates of reflector curvature and rotation: Geophysics, **71**, no. 5, P41–P51, doi: 10.1190/1.2242449.

Antoine, B., and B. Frederic, 2016, Evaluation of in-situ stress environment in the Utica play and implications on completion design and well performance: Unconventional Resources Technology Conference, URTeC: 2429699.

Chopra, S., and K. J. Marfurt, 2007, Seismic attributes for prospect identification and reservoir characterization: SEG, Geophysical Development Series.

Chopra, S., and K. J. Marfurt, 2008, Gleaning meaningful information from seismic attributes: First Break, **26**, 43–53, doi: 10.3997/1365-2397.2008012.

Chopra, S., R. K. Sharma, J. Keay, and K. J. Marfurt, 2012, Shale gas reservoir characterization workflows: 82nd Annual International Meeting, SEG, Expanded Abstracts, doi: 10.1190/segam2012-1344.1.

Cocklin, J., 2015, Shale daily, published on 14 July 2015, http://www.naturalgasintel.com/articles/102982-wvu-study-finds-bounty-of-utica-shale-natgas-waiting-for-production, accessed on 18 February 2017.

Downing, B., and D. Livingston, 2015, Sharp decline in well production typical in Ohio's Utica shale, Ohio.com, published on January 4, 2015, https://www.ohio.com/akron/business/sharp-declines-in-well-production-typical-in-ohio-s-utica-shale, accessed on 10 October 2017.

EIA Report, 2017, Utica shale play, Geology review, https://www.eia.gov/maps/pdf/UticaShalePlayReport_April2017.pdf, accessed on 10 October 2017.

Grieser, B., and J. Bray, 2007, Identification of production in unconventional reservoirs: SPE Production and Operations Symposium, SPE, 106623.

Hansen, M. C., 1997, The geology of Ohio — The Ordovician, Ohio geology, Ohio division of geological survey, http://jrscience.wcp.miamioh.edu/downloads/Ordoviciangeology.pdf, accessed on 18 February 2017.

Jefferies, 2013, Utica/Point Pleasant shale play update, http://www.jefferies.com/CMSFiles/Jefferies.com/files/Conferences/Utica%20Shale%20Point%20Pleasant%20Play%20Update%20vF.pdf, accessed on 21 February 2017.

Kirschbaum, M. A., C. J. Schenk, T. A. Cook, R. T. Ryder, R. R. Charpentier, T. R. Klett, S. B. Gaswirth, M. E. Tennyson, and K. J. Whidden, 2012, Assessment of undiscovered oil and gas resources of the Ordovician Utica shale of the Appalachian Basin Province, 2012: U.S. Geological Survey Fact Sheet 2012–3116, 6.

Marfurt, K. J., 2006, Robust estimates of reflector dip and azimuth: Geophysics, **71**, no. 4, P29–P40, doi: 10.1190/1.2213049.

Mariani, K., 2013, EnerVest's long-held strategy reaps new rewards in burgeoning Utica Play, American Oil and Gas Reporter, February issue, http://www.aogr.com/magazine/editors-choice/enervests-long-held-strategy-reaps-new-rewards-in-burgeoning-utica-play, accessed on 18 February 2017.

Murphy, E., M. Warner, and B. Sarmah, 2013, A workflow to evaluate porosity, mineralogy, and TOC in the Utica-Point Pleasant shale play: SPE Eastern Regional Meeting, SPE, 165682.

Patchen, D. G., and K. M. Carter, eds., 2012, A geologic play book for Utica shale Appalachian Basin Exploration, http://marcellusdrilling.com/2015/07/wvu-research-shock-finding-utica-is-as-big-as-marcellus/, accessed on 27 March 2017.

Patchen, D. G., and K. M. Carter, eds., 2015, A geologic play book for Utica shale Appalachian basin exploration: Final report of the Utica Shale Appalachian basin exploration consortium, 187, http://www.wvgs.wvnet.edu/utica, accessed on 18 February 2017.

Pickett, A., 2015, Operators finding record wells and new frontiers in Marcellus/Utica, American Oil and Gas Reporter, http://www.rangeresources.com/docs/default-source/factsheets/aogr-recordwells.pdf?sfvrsn=2, accessed on 10 October 2017.

Ray, A. K., and S. Chopra, 2015, More robust methods of low-frequency model building for seismic impedance inversion: 85th Annual International Meeting, SEG, Expanded Abstracts, 3398–3402.

Ray, A. K., and S. Chopra, 2016, Building more robust low-frequency models for seismic impedance inversion: First Break, **34**, 29–34, doi: 10.3997/1365-2397.2016005.

Rickman, R., M. J. Mullen, J. E. Petre, W. V. Grieser, and D. Kundert, 2008, A practical use of shale petrophysics for stimulation design optimization: All shale plays are not clones of the Barnett shale: SPE Annual Technical Conference and Exhibition, SPE, 115258.

Sharma, R. K., and S. Chopra, 2016, Identification of sweet spots in shale reservoir formations: First Break, **34**, 39–47, doi: 10.3997/1365-2397.2016012.

Wickstrom, L., 2013, Geology and activity of the Utica-Point Pleasant of Ohio, http://www.searchanddiscovery.com/documents/2013/10490wickstrom/ndx_wickstrom.pdf, accessed on 18 February 2017.

Biographies and photographs of the authors are not available.